minerals

Article

Fractal Dimension Analysis of Pores in Coal Reservoir and Their Impact on Petrophysical Properties: A Case Study in the Province of Guizhou, SW China

Wei Fu [1], Wangshui Hu [1,*], Tongsheng Yi [2], Oumar Ibrahima Kane [1], Manting Zhang [1] and Xin Huang [1]

[1] School of Geosciences, Yangtze University, Wuhan 430100, China
[2] Guizhou Engineering Technology Research Center for Coalbed Methane and Shale Gas, Guiyang 550009, China
* Correspondence: hws@yangtzeu.edu.cn

Abstract: Coal is a complex, porous medium with pore structures of various sizes. Therefore, it is difficult to accurately describe the characteristics of pore structure by using the traditional geometry method. The results from the present investigation suggest that the porous media system of the coal reservoir has obvious fractal characteristics at different scales. To study the complexity of the pores in the coal reservoir, 27 coal samples from Guizhou, SW China were studied. The fractal dimensions of coal pores were calculated, and the fractal dimension of a pore in a coal reservoir can be classified into two types: percolation and diffusion. The comprehensive fractal dimension can be obtained using the weighted summation method and the pore volume fraction of different fractal segments as the weight. The percolation fractal dimensions (D_p) of coal samples are between 2.88 and 3.12, the diffusion fractal dimensions (D_d) are between 3.57 and 3.84, and the comprehensive fractal dimensions (D_t) are between 3.05 and 3.63. The D_d values of all coal samples are all larger than the D_p values, which indicates that the random distribution and complexity of diffusion pores in coal are stronger than those of the percolation pores. The percolation fractal dimension decreases as the maturity degree increases, whereas the diffusion and comprehensive fractal dimensions increase. The diffusion pore volume fraction and total pore volume are all highly correlated with the comprehensive and diffusion fractal dimensions, respectively. The correlation between the comprehensive fractal dimension, diffusion pore volume fraction, and coal reservoir porosity is negative exponential, whereas the correlation between the total pore volume and coal reservoir porosity is positive linear. In comparison with the percolation and diffusion fractal dimensions, the comprehensive fractal dimension is better suited for characterizing the permeability of coal reservoirs. The fractal analysis of this paper is beneficial for understanding the relationship between the fractal characteristics of coal pores and properties.

Keywords: Southwestern China; coal pores; mercury injection experiment; fractal dimension; petrophysical properties

Citation: Fu, W.; Hu, W.; Yi, T.; Kane, O.I.; Zhang, M.; Huang, X. Fractal Dimension Analysis of Pores in Coal Reservoir and Their Impact on Petrophysical Properties: A Case Study in the Province of Guizhou, SW China. *Minerals* **2022**, *12*, 1425. https://doi.org/10.3390/min12111425

Academic Editor: Samintha Perera

Received: 16 September 2022
Accepted: 2 November 2022
Published: 10 November 2022

1. Introduction

Coal is a disordered heterogeneous pore medium; the pore structure is directly related to methane adsorption and fluidity [1,2]. The existing research shows that the composition of coal is critical to determine the characteristics of coal reservoirs [3,4]. Southwestern China owns one of the largest coal-producing fields in the country [5,6]. The Longtan Formation of Guizhou province in this region contains abundant coal resources and extremely rich coalbed methane (CBM) resources [7,8]. However, the complex geological conditions in this area seriously restrict the development of coalbed methane production [9,10], with one of the most significant factors being the structure of the pores [11,12]. The pores and fissures of coal reservoirs are important spaces for coalbed methane adsorption, migration, and accumulation [13,14]. It plays an important role in controlling the adsorption capacity and the permeability of coal [15].

The pore characteristics of coal are highly heterogeneous [16,17]. It is difficult to accurately describe and analyze the complexity of the pore structure by using traditional geometry methods [18,19]. Most scholars tend to use fractal mathematical methods to describe its characteristics [20,21]. Different scholars have carried out significant research on the selection of fractal scale, calculation of fractal dimension, and physical property characterization of fractal geometric parameters of coal reservoir pores, but the conclusions are quite different [22,23]. This is because the pore systems of coal reservoirs in different areas are very different due to differences in metamorphic degree and reservoir physical properties [24,25]. It further indicates the complexity and particularity of the pore system in coal reservoirs [26,27].

In recent years, some scholars have studied pore characteristics, geological controlling factors of coal reservoirs [1,28], and the fractal characteristics of pores on a certain scale in some mining areas of the southwestern part of China [29–31]. However, comprehensive fractal research of the reservoir is seldom involved. This paper uses typical bituminous coal samples and typical anthracite samples in Southwestern China as the research object. In this study, 27 coal samples were collected, and vitrinite reflectance (R_o) measurement, coal proximate analysis, and mercury injection tests were performed on all samples. Based on the results of the equipment, the fractal dimension was calculated. Afterward, the relationship between different parameters was studied. The primary goals of this study were: (1) quantitatively study the fractal characteristics of different pore sizes in coal reservoirs by using fractal theory, and calculate their fractal dimension in sections; (2) discuss the internal relationship of fractal geometric parameters, such as piecewise fractal dimension and comprehensive fractal dimension, and their effects on porosity and permeability. The study is beneficial for better understanding the relationship between fractal characteristics of coal pores and petrophysical properties.

2. Experiment and Methodology

2.1. Equipment and Materials

In order to study the fractal characteristics of coal pores and their impact on the petrophysical properties, a total of 27 coal samples were collected from Longtan Formation in Guizhou province, SW China. A total of 23 of the samples are bituminous coal and 4 are anthracite. The collection process of the samples followed the Standard Method of China (GB/T 19222-2003). All coal samples were obtained from CBM parameter wells or working surfaces of underground mines from 8 coalfields. Some permeability values of coal beds were acquired by an injection test. The statistical results show that the permeability of the coal beds in this region ranges between 0.027×10^{-15} m^2 and 0.573×10^{-15} m^2; this suggests that the permeability of coal beds in this region is relatively low [32–34].

Vitrinite reflectance (R_o) measurement, coal proximate analysis, and mercury injection tests were performed on all samples. The measurement of R_o followed the National Standards of China (GB/T 8899-2013), and the proximate analysis followed the test method ISO 17246-2010. We used the mercury injection method to test the porosity of the samples. The instrument was Autopore IV 9500, which was produced by Micromeritics. To avoid the negative effects of mineral impurity and other factors in the sample preparation process, the samples were crushed into particles with a dimension of 2–4 mm. The mercury injection test shows the distribution of pores diameter in soil based on the fact that non-infiltrative liquid will not flow into solid pores without pressure. The pressure required for liquid injection into the pores is based on the Washburn equation [35,36]. The relationship between the pressure and the volume of mercury was obtained from the mercury injection test. The Washburn equation was used to find the corresponding equivalent diameter through pressure, from which the pore distribution of coal was obtained [37,38]. Additionally, we excluded the results with apertures larger than 100,000 nm as these obviously oversized pores are not the pore system of the sample itself. The porosity measurements followed the Petroleum Industry Standard of China SY/T 6385-1999.

2.2. Methodology

Fractal dimension is an important parameter to describe fractal characteristics, which describes the complexity or roughness of the coal surface. Many scholars have deduced the fractal dimension of the pore volume of coal reservoirs according to the basic theory of fractals [34,39,40]. Based on the mercury injection data, Equation (1) was utilized to determine the relationship between mercury injection volume and mercury injection pressure in coal samples [11,41,42] and is as follows:

$$\lg\left(\frac{dV_p}{dP}\right) \propto (D-4)\lg P \quad (1)$$

where P is the external pressure in the process of mercury injection, in MPa; dVp is the pore volume increment of the corresponding pressure increment dP, in cm^3/g; and D is the fractal dimension of coal pore volume, and is dimensionless.

Through the scatter plot of $\lg\left(\frac{dV_p}{dP}\right)$ and lg P, one or more linear relationship segments will appear in the graph using the mercury injection test data of coal samples. As long as there is a linear relationship between $\lg\left(\frac{dV_p}{dP}\right)$ and lg P, the pore distribution of the corresponding segment conforms to the fractal characteristics, and the fractal dimension of the segment $D = 4 + K$ can be obtained, where K is the slope of the line [14,18,43].

Existing research on the fractal dimension of coal pores has shown that different pore sizes in coal have fractal dimension characteristics in the subsection [3,23,44]. In the study of mercury injection fractals of coal samples in the Bide–Santang Basin in Southwestern China, it has been found that there are three kinds of pore systems in coal samples, namely large pores between particles of coal matrix >6000 nm, transition pores in coal matrix particles between 6000 and 73 nm, and small/micropores in coal matrix particles <73 nm [45]. They correspond to three different pore fractions, which were called the fractal dimension of large pores (D_1), the fractal dimension of transitional pores (D_2), and the fractal dimension of small/micropores (D_3) [45–47]. The mercury injection fractal of a large number of coal samples collected from different regions of China in different geological times and coal grades were studied based on the diffusion and percolation characteristics of coal bed methane [1,48,49]. The aforementioned study divided the coal pores into percolation pores (>65 nm) and diffusion pores (<65 nm). Jiang et al. studied the samples from West China and found that there are two different fractal characteristics of coal reservoir pores, namely the fractal dimension of the larger pore stage as the percolation fractal dimension and the fractal dimension of the smaller pore stage as the diffusion fractal dimension [50]. The fractal dimension of different pore sizes is related to the physical properties of the reservoir, but it is difficult to represent the complexity of coal [51,52]. Ren et al. proposed a method to study the fractal dimension of coal samples. In this method, the ratio of different pore sizes was taken as the weight coefficient, and the comprehensive fractal dimension was obtained by the weighted summation of the fractal dimension of different pore size segments. The calculation equation is as follows:

$$D_t = \sum D_i T_i \quad (2)$$

where D_t is the comprehensive fractal dimension of coal, D_i is the fractal dimension corresponding to the pore size segment, T_i is the pore size ratio corresponding to the pore size segment, and i is the pore size segment code.

3. Results

3.1. Results of Conventional Coal Test

Table 1 shows the results of the experiments. The R_o of bituminous coals ranges from 1.05% to 1.95%, with an average value of 1.60%. The results of the proximate analysis show that the moisture content (ad), ash yield (Ad), and volatile matter (daf) range from 0.69 to 1.680% (average 0.94%), 12.53 to 28.62% (average 22.18%), and 15.94 to 33.48% (average 22.90%).

Table 1. Test results of coal samples.

Sample Nos.	Coal Rank	R_o/%	Proximate and Ultimate (wt%)			Porosity (%)	Total Pore Volume (mL/g)
			M_{ad}	A_d	V_{daf}		
M_1	Bituminous coal	1.05	0.75	16.28	33.48	4.01	0.0284
M_2		1.07	1.68	25.17	31.80	3.85	0.0236
M_3		1.13	1.52	24.83	30.85	5.68	0.0412
M_4		1.09	0.95	20.48	32.97	3.27	0.0244
M_5		1.10	0.88	19.34	29.18	4.22	0.0251
S_1		1.45	1.06	21.87	23.98	3.74	0.0261
S_2		1.22	1.14	19.27	24.59	4.02	0.0248
S_3		1.43	1.28	21.39	22.48	3.84	0.0257
S_4		1.24	1.85	20.14	24.26	3.97	0..0277
F_1		1.67	0.95	18.67	21.87	3.78	0.0191
F_2		1.54	1.25	19.38	20.89	3.68	0.0210
F_3		1.68	0.85	21.08	18.92	3.47	0.0199
F_4		1.42	1.33	19.38	19.46	4.89	0.0223
W_1		1.81	0.71	26.15	19.38	9.25	0.0538
W_2		1.85	0.98	28.62	18.89	9.14	0.0634
W_3		1.93	0.69	12.53	15.94	5.37	0.0402
W_4		1.84	0.78	18.78	17.96	6.47	0.0581
W_5		1.79	0.93	20.96	20.39	7.25	0.0495
W_6		1.92	0.73	14.69	18.88	5.77	0.0513
G_1		1.95	0.71	28.14	17.82	3.64	0.0227
G_2		1.85	0.92	18.98	20.68	5.87	0.0428
G_3		1.92	1.24	24.39	17.11	4.26	0.0328
G_4		1.89	0.85	20.64	20.47	5.84	0.0215
H_1	Anthracite	3.31	2.30	21.38	7.88	3.41	0.0213
H_2		3.24	2..14	20.86	10.96	4.95	0.0328
H_3		3.14	2.02	17.39	12.85	3.99	0.0259
H_4		3.30	1.95	20.18	8.89	4.12	0.027

R_o: vitrinite reflectance, %; M_{ad}: moisture (air-dried basis); A_d (dry basis); V_{daf} (dry ash-free basis).

3.2. Results of Mercury Intrusion

The mercury intrusion curves for different samples are shown in Figure 1. All curves show the hysteresis loop phenomenon. The mercury injection curves in the study area were divided into two types. Type I (Figure 1a) shows that when low pressure is increased the mercury intake increases significantly with the increase in mercury injection pressure, and shows obvious hysteresis, indicating that there are more open pores and good connectivity.

Type II (Figure 1b) shows that with the continuous increase in mercury intrusion pressure, the mercury intrusion curve continues to rise, indicating that the pores of all scales are distributed and open.

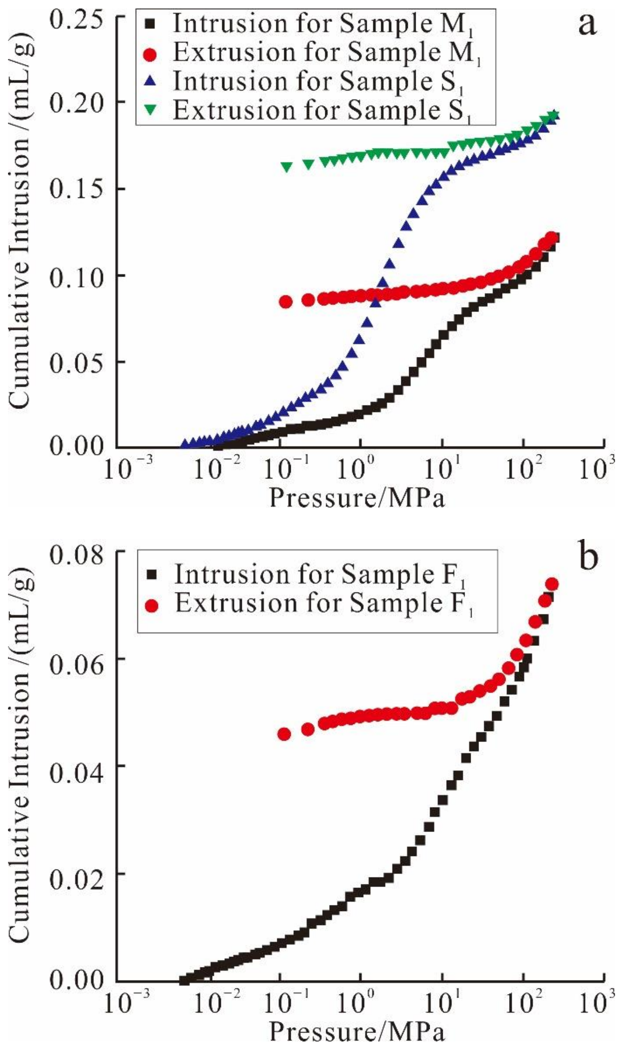

Figure 1. Mercury intrusion curves for different samples. (**a**) Sample M_1 & Sample S_1; (**b**) Sample F_1.

3.3. Results of Fractal Dimension Calculation

According to Equation (1), the relation diagram of lg(dV_P/dP) and lg$P$ was drawn from mercury injection data of coal samples (Figure 2). The fractal curve can be divided into two different linear sections: a low-pressure section and a high-pressure section. The linear regression correlation coefficients of each section are all above 0.90. This indicates that there are two different pore systems in the coal samples. The low-pressure section corresponds to a large pore diameter section, and the high-pressure section corresponds to a small pore diameter section. In this paper, the fractal dimension of the larger pore section is called the percolation fractal dimension (D_{p}), and the fractal dimension of the smaller pore section is called the diffusion fractal dimension (D_{d}).

It can be observed in Figure 2 that the graph from lg$P$ and lg(dV_P/dP) shows two distinct lines and lg$P$ of the yielding points is between 1.1 and 1.4. The corresponding coal pore radius is between 54 and 85 nm, with an average of 65 nm. This phenomenon is consistent with the study of Fu et al. (2005) which has been shown in the methodology. In this study, we followed the classification scheme of Fu et al. (2005) and set 65 nm as the boundary of percolation pores and diffusion pores.

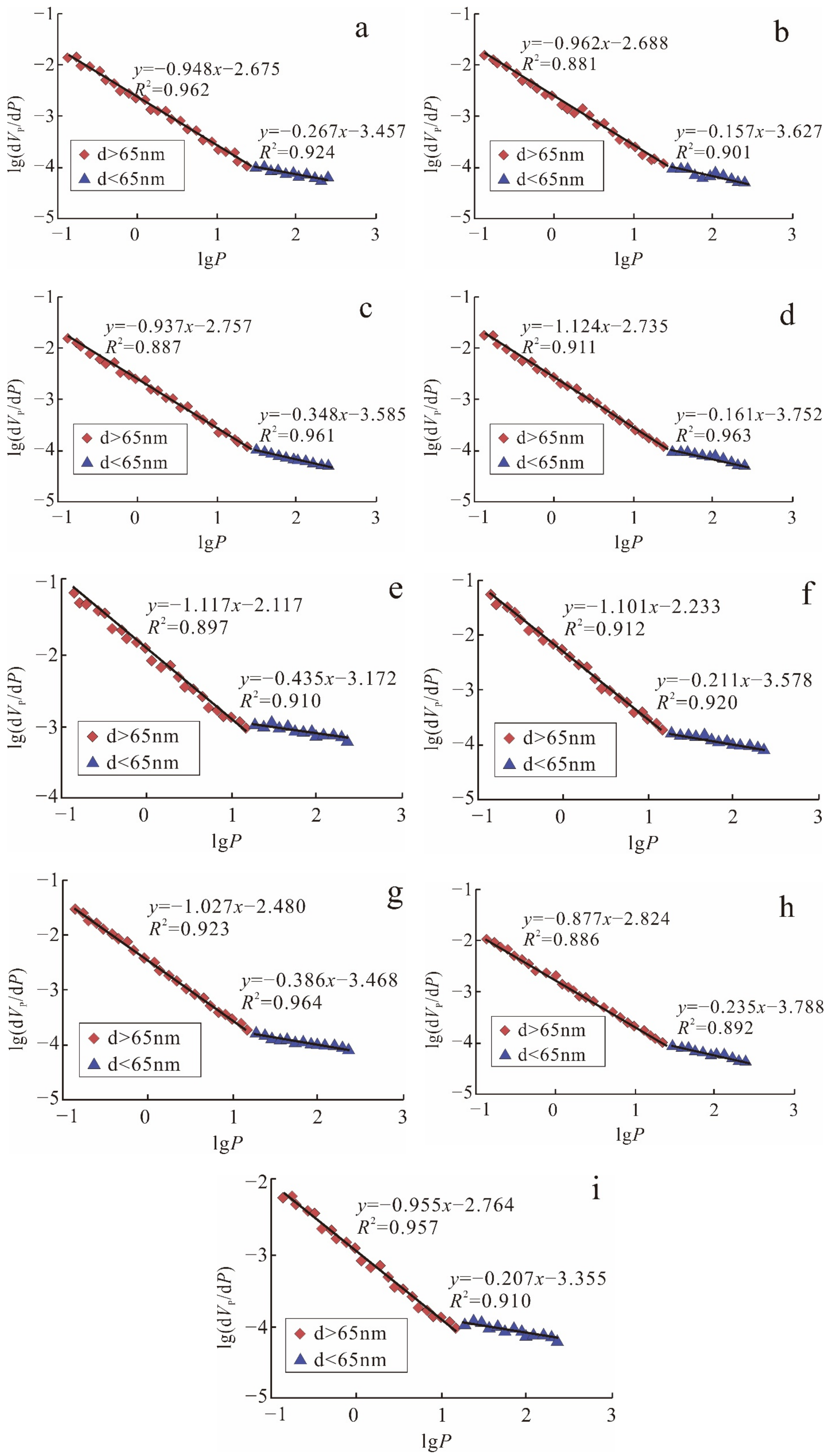

Figure 2. Plots of $\lg(dV_P/dP)$ as a function of $\lg P$ for selected samples (**a**): Sample M_1; (**b**): Sample M_2; (**c**): Sample S_1; (**d**): Sample F_1; (**e**): Sample W_1; (**f**): Sample W_2; (**g**): Sample W_3; (**h**): Sample G_1; (**i**): Sample H_1.

Table 2 lists the fractal dimension, correlation coefficient, and pore size ratio of some coal samples with different pore sizes. According to Equation (2), the comprehensive fractal dimension (D_t) of each coal sample is obtained as a weighted average.

Table 2. Calculation results of fractal dimension of some coal samples.

Sample Nos.	Percolation Pore Segment				Diffusion Pore Segment				D_t
	Linear Fitting Equation	R^2	D_p	Pore Size Ratio/%	Linear Fitting Equation	R^2	D_d	Pore Size Ratio/%	
M_1	$Y = -0.948x - 2.675$	0.96	3.05	44	$Y = -0.267x - 3.457$	0.92	3.73	56	3.43
M_2	$Y = -0.962x - 2.688$	0.88	3.04	35	$Y = -0.157x - 3.627$	0.90	3.84	65	3.56
M_3	$Y = -0.958x - 2.635$	0.81	3.04	41	$Y = -0.257x - 3.659$	0.87	3.74	59	3.46
M_4	$Y = -0.922x - 2.578$	0.84	3.08	39	$Y = -0.195x - 3.561$	0.82	3.81	61	3.52
M_5	$Y = -0.968x - 2.458$	0.80	3.03	42	$Y = -0.281x - 3.486$	0.84	3.72	58	3.43
S_1	$Y = -0.937x - 2.757$	0.89	3.06	37	$Y = -0.348x - 3.585$	0.96	3.65	63	3.43
S_2	$Y = -0.952x - 2.582$	0.81	3.05	38	$Y = -0.385x - 3.518$	0.91	3.62	62	3.40
S_3	$Y = -0.901x - 2.747$	0.85	3.10	35	$Y = -0.315x - 3.685$	0.82	3.69	65	3.48
S_4	$Y = -0.978x - 2.638$	0.88	3.02	41	$Y = -0.341x - 3.725$	0.84	3.66	59	3.40
F_1	$Y = -1.124x - 2.735$	0.91	2.88	32	$Y = -0.161x - 3.752$	0.96	3.84	68	3.53
F_2	$Y = -1.114x - 2.582$	0.88	2.89	39	$Y = -0.158x - 3.857$	0.84	3.84	61	3.47
F_3	$Y = -1.125x - 2.758$	0.81	2.88	35	$Y = -0.181x - 3.581$	0.86	3.82	65	3.49
F_4	$Y = -1.117x - 2.856$	0.84	2.88	37	$Y = -0.178x - 3.893$	0.90	3.82	63	3.47
W_1	$Y = -1.117x - 2.117$	0.90	2.88	76	$Y = -0.435x - 3.172$	0.99	3.57	24	3.05
W_2	$Y = -1.101x - 2.333$	0.91	2.90	69	$Y = -0.211x - 3.578$	0.92	3.79	31	3.17
W_3	$Y = -1.027x - 2.480$	0.92	2.97	48	$Y = -0.386x - 3.468$	0.96	3.61	52	3.31
W_4	$Y = -1.146x - 2.500$	0.90	2.85	65	$Y = -0.582x - 3.573$	0.87	3.42	35	3.05
W_5	$Y = -1.085x - 2.581$	0.88	2.92	58	$Y = -0.379x - 3.458$	0.80	3.62	42	3.21
W_6	$Y = -1.055x - 2.494$	0.82	2.95	49	$Y = -0.375x - 3.483$	0.96	3.63	51	3.29
G_1	$Y = -0.877x - 2.824$	0.89	3.12	34	$Y = -0.235x - 3.788$	0.89	3.77	66	3.55
G_2	$Y = -0.925x - 2.458$	0.87	3.08	38	$Y = -0.285x - 3.581$	0.89	3.72	62	3.47
G_3	$Y = -0.895x - 2.594$	0.81	3.11	42	$Y = -0.246x - 3.673$	0.85	3.75	58	3.48
G_4	$Y = -0.880x - 2.765$	0.79	3.12	36	$Y = -0.249x - 3.657$	0.90	3.75	64	3.52
H_1	$Y = -0.955x - 2.764$	0.96	3.05	22	$Y = -0.207x - 3.355$	0.91	3.79	78	3.63
H_2	$Y = -0.924x - 2.724$	0.90	3.08	38	$Y = -0.182x - 3.278$	0.81	3.82	62	3.54
H_3	$Y = -0.975x - 2.681$	0.85	3.03	32	$Y = -0.214x - 3.281$	0.86	3.79	68	3.54
H_4	$Y = -0.968x - 2.588$	0.80	3.03	29	$Y = -0.193x - 3.589$	0.90	3.81	71	3.58

The results in Table 2 show that the percolation fractal dimensions (D_p) of coal samples are between 2.88 and 3.12, the diffusion fractal dimensions (D_d) are between 3.57 and 3.84, and the comprehensive fractal dimensions (D_t) are between 3.05 and 3.63. The D_d of all coal samples are all larger than D_p, which indicates that the random distribution and complexity of diffusion pores in coal are stronger than that of the percolation pores.

4. Discussion

4.1. The Validity of the Calculation Results

According to the theory of fractal geometry, the fractal dimension of a porous solid should be between 2.0 and 3.0 in general; however, some fractal dimensions in Table 2 exceed 3. Some scholars have found that if the compression deformation of a porous solid occurs under high pressure, the results of the fractal dimension may be larger than 3.0 [51,53].

Yang et al. (2021) and Cai et al. (2018) studied the compressibility of the coal matrix and its impact on the results of MIP. They provided a semi-empirical Tait equation to correct the results of MIP [54,55]. However, the coal rank and proximate of the samples tested in this work are multiple, which indicated that the compressibility of different samples varies greatly. Therefore, it is difficult to correct the fractal dimension by a unified method. Many scholars have repeatedly obtained the result that the fractal dimension is larger than 3. Therefore, although the calculation results of partial fractal dimension are greater than 3, under the same test conditions, a fractal dimension greater than 3.0 is an effective index to characterize the physical properties of the reservoir.

4.2. Relationship between Fractal Dimensions and Vitrinite Reflectance

By comparing the relationship between the fractal dimension of samples and the degree of maturity, it can be found that the D_p decreases gradually with the increase in the maturity degree (Figure 3), while the D_d and D_t increase with the increase in the maturity degree (Figures 4 and 5). This phenomenon happens because, with the increase in the metamorphic degree, the percolation pores with a larger pore size in the coal are gradually compacted and homogenized, and many irregular diffusive pores with a small pore size are formed during the process of structural compression and compaction of percolation pores. The comprehensive fractal dimension (D_t) increases with the metamorphic degree, which has the same trend as the diffusion fractal dimension (D_d), indicating that the complexity of the coal pores mainly depends on the complexity of diffusion pores (D_d).

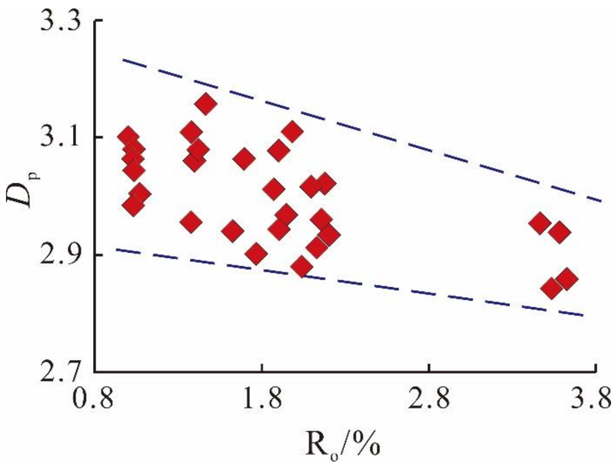

Figure 3. Relationship between percolation fractal dimension (D_p) and vitrinite reflectance (R_o).

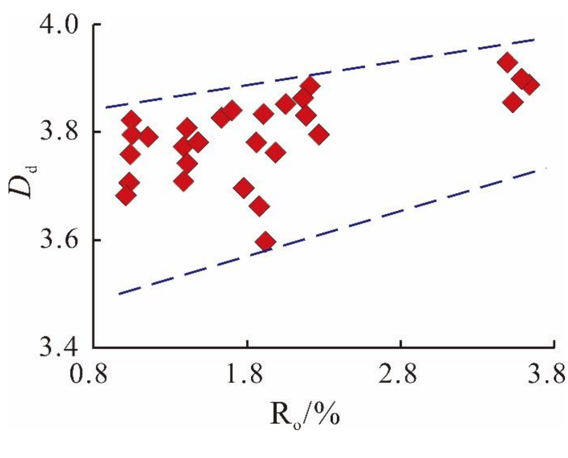

Figure 4. Relationship between diffusion fractal dimension (D_d) and vitrinite reflectance (R_o).

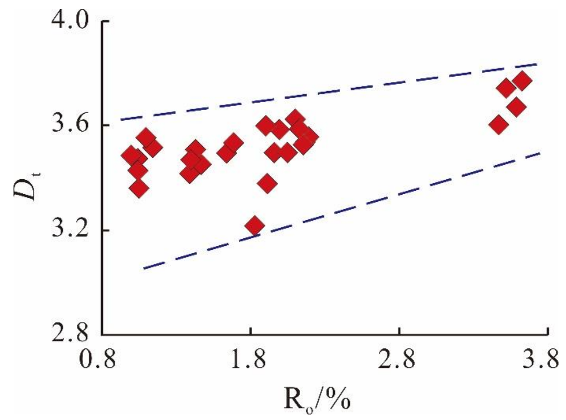

Figure 5. Relationship between comprehensive fractal dimension (D_t) and vitrinite reflectance (R_o).

4.3. Relationship between Volume Fraction of Diffusion Pores and Fractal Dimensions

The investigation of each fractal parameter shows that the diffusion pore volume fractions are poorly correlated with percolation fractal dimension (Figure 6), while it has a good positive linear correlation with diffusion fractal dimension and comprehensive fractal dimension, especially when the linear regression number of diffusion pore volume fraction and comprehensive fractal dimension reaches 0.951 (Figures 7 and 8). It shows that the coal with a smaller volume fraction of diffusion pores has less complexity in the pores. This phenomenon preliminarily shows that the diffusion pore volume fractions are important geometric parameters that indirectly characterize the complexity of coal.

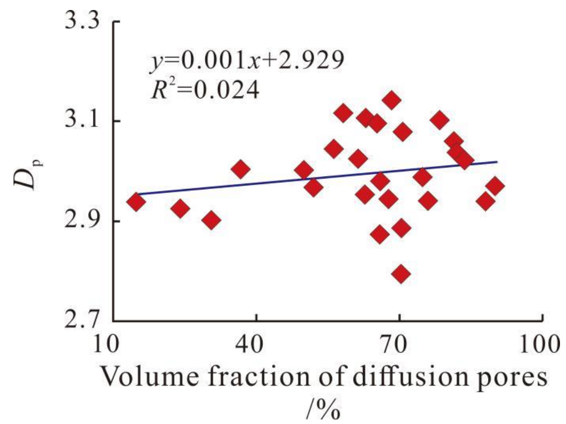

Figure 6. Relationship between volume fraction of diffusion pores and percolation fractal dimension (D_p).

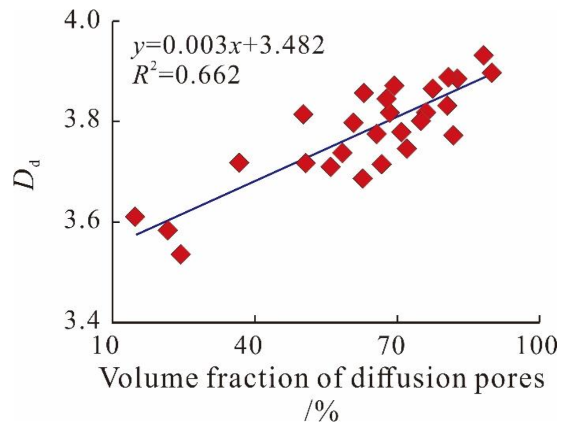

Figure 7. Relationship between volume fraction of diffusion pores and diffusion fractal dimension (D_d).

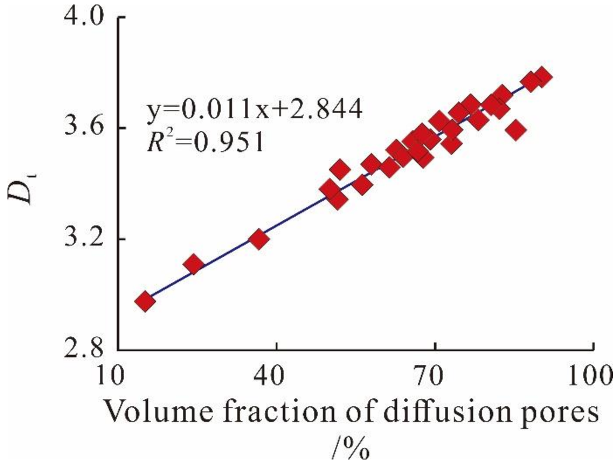

Figure 8. Relationship between volume fraction of diffusion pores and comprehensive fractal dimension (D_t).

4.4. Relationship between Fractal Dimensions and Total Pore Volume

The following figures illustrate that the total pore volume is poorly correlated with the percolation fractal dimension (D_p) (Figure 9), and inversely proportional to the diffusion fractal dimension (D_d) (Figure 10) and comprehensive fractal dimension (D_t) (Figure 11), indicating that increasing total pore volume is beneficial in reducing the complexity of coal pores and making the pore surface of coal, especially the diffusion pore surface, smoother. By comparing the correlation coefficients of the fractal parameters, it is found that the comprehensive fractal dimension has the highest correlation coefficients with each geometrical parameter, the correlation coefficient between diffusion fractal dimension and geometrical parameters is smaller, and the correlation coefficients between percolation fractal dimension and geometrical parameters were very low (less than 0.1) (Figure 9). The correlation between the percolation fractal dimension and the single geometric parameter is not significant. This indicates that the factors affecting the surface roughness of the percolation pore are very complex, and any single geometric parameter is difficult to effectively characterize the complexity of the percolation pore.

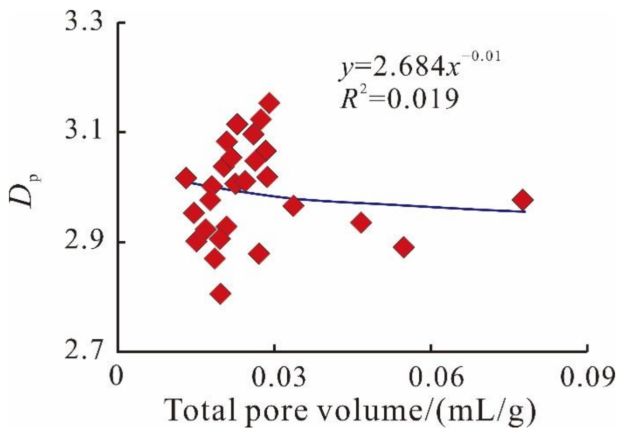

Figure 9. Relationship between total pore volume and percolation fractal dimension (D_p).

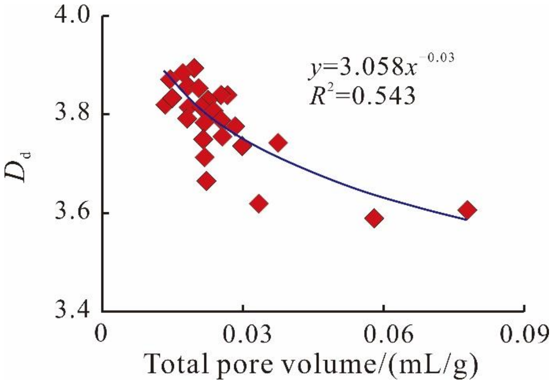

Figure 10. Relationship between total pore volume and diffusion fractal dimension (D_d).

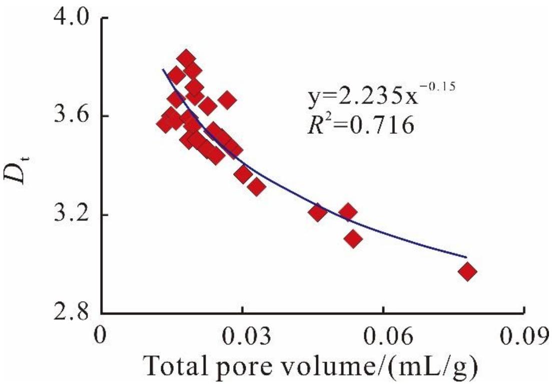

Figure 11. Relationship between total pore volume and comprehensive fractal dimension (D_t).

4.5. Relationship between Fractal Parameters and Porosity

Porosity is an important parameter to describe the petrophysical properties of coal reservoirs. In this study, almost all of the samples were below 5%. The comprehensive fractal dimension of coal samples has a negative power exponential correlation with porosity (Figure 12). This phenomenon can be the result of an increased pore network complexity that leads to poor pore connectivity, which results in lower porosity values. According to the previous analysis, the volume fraction of diffusion pores and total pore volume correlate with the comprehensive fractal dimension. Therefore, they are important fractal geometric parameters in order to characterize the complexity of coal reservoirs. By analyzing the correlation between these three parameters and porosity, the pore volume of fraction diffusion decreases with the increase in porosity (Figure 13). This shows that the comprehensive fractal dimension and the volume fraction of diffusion pores can indirectly characterize coal porosity.

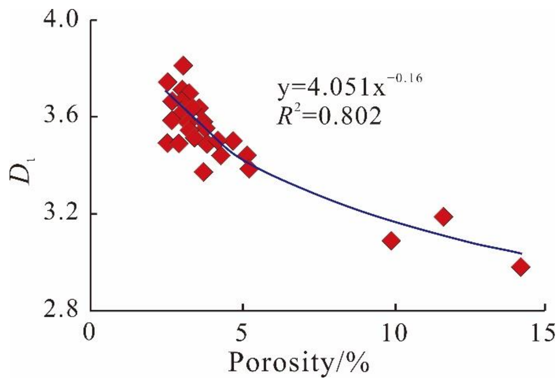

Figure 12. Relationship between porosity and comprehensive fractal dimension (D_t).

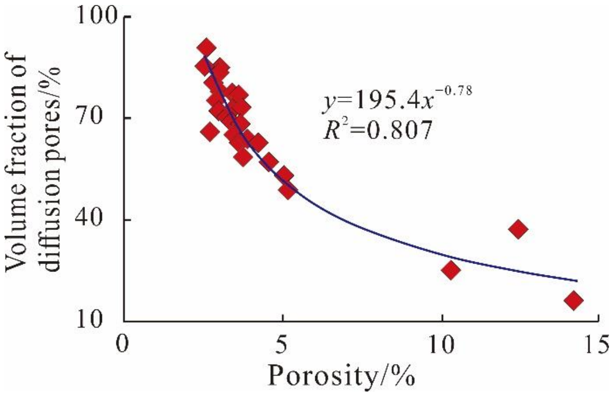

Figure 13. Relationship between porosity and volume fraction of diffusion pores.

4.6. Brief Summary

According to the research above, this paper studied the advantages of the comprehensive fractal dimension of coal pores in detail. The fractal characteristics of coal pores were discussed. Through the establishment of the comprehensive fractal dimension, the petrophysical properties of coal were analyzed.

The result of the research shows that the comprehensive fractal dimension can better reflect the complexity of coal pores. This conclusion is consistent with the conclusions of other scholars [18,20]. Additionally, the result also shows that the diffusion fractal dimension has a greater reflection on the pore complexity of coal pores than the percolation fractal dimension. This phenomenon can also be supported by other scholars [2,8,56].

The shortage of this paper is the lack of study on the permeability, as the complexity of coal pores has an important effect on the permeability of coal reservoirs [27,57,58].

5. Conclusions

Based on the fractal geometry and mercury injection test data, the complexity of pores in collected samples from the Longtan Formation in Guizhou province, SW China, was studied. The pore fractal dimension of the coal reservoir is divided into the percolation fractal dimension and the diffusion fractal dimension. In addition, the comprehensive fractal dimension of the coal sample can be obtained by the weighted summative method.

The percolation fractal dimension decreases as the metamorphic degree increases, whereas the diffusion fractal dimension and comprehensive dimension both increase, and the complexity of diffusion pores has a greater effect on the complexity of pores in coal.

Indirectly, the complexity of coal pores can be determined by the fractal boundary, volume fraction of diffusion pores, and total pore volume. Correlation coefficients between the parameters and the comprehensive fractal dimension are greater than those between the parameter and the diffusion fractal dimension, and there is no obvious correlation between the parameters and the percolation fractal dimension.

The comprehensive fractal dimension, fractal boundary, diffusion pore volume fraction, and total pore volume can all quantitatively reflect the porosity of the coal reservoir. The comprehensive fractal dimension, fractal boundary, and diffusion pore volume fraction all decrease with the increasing porosity of coal. The total pore volume increases linearly in proportion to the coal reservoir porosity.

Author Contributions: Conceptualization, W.H.; methodology, W.F.; validation, W.F., M.Z. and X.H.; formal analysis, W.F.; investigation, W.F.; resources, W.H.; data curation, M.Z.; writing—original draft preparation, W.F.; writing—review and editing, O.I.K.; visualization, M.Z.; supervision, W.H.; project administration, T.Y.; funding acquisition, W.H. All authors have read and agreed to the published version of the manuscript.

Funding: This research received no external funding or This research was funded by National Major Science and Technology Projects of China grant number 2016ZX05034-004 and The APC was funded by Yangtze University.

Data Availability Statement: The data that support the findings of this study are available from the corresponding author upon reasonable request.

Conflicts of Interest: The authors declare no conflict of interest.

References

1. Zhao, S.; Chen, X.; Li, X.; Qi, L.; Zhang, G. Experimental Analysis of the Effect of Temperature on Coal Pore Structure Transformation. *Fuel* **2021**, *305*, 121613. [CrossRef]
2. Nie, A.; Mei, S.; Guan, D.; Wu, P.; Zhang, Z. A Study on the Genetic Relations between Permian Longtan Formation Coal Series Strata and Carlin-Type Gold Deposits, Southwestern Guizhou Province, China. *Chin. J. Geochem.* **2008**, *27*, 291–298. [CrossRef]
3. Zhao, Y.; Sun, Y.; Liu, S.; Wang, K.; Jiang, Y. Pore Structure Characterization of Coal by NMR Cryoporometry. *Fuel* **2017**, *190*, 359–369. [CrossRef]
4. Li, Y.; Yang, J.; Pan, Z.; Tong, W. Nanoscale Pore Structure and Mechanical Property Analysis of Coal: An Insight Combining AFM and SEM Images. *Fuel* **2020**, *260*, 116352. [CrossRef]
5. Li, B.; Zhuang, X.; Li, J.; Querol, X.; Font, O.; Moreno, N. Enrichment and Distribution of Elements in the Late Permian Coals from the Zhina Coalfield, Guizhou Province, Southwest China. *Int. J. Coal Geol.* **2017**, *171*, 111–129. [CrossRef]
6. Li, Z.; Gao, W.; Li, X. Correlations of Permeability and Geological Characteristics Based on Mercury Intrusion Data and Hierarchical Statistical Models: A Case Study. *J. Energy Resour. Technol.* **2020**, *142*, 123004. [CrossRef]
7. Bi, C.; Zhang, J.; Shan, Y.; Hu, Z.; Wang, F.; Chi, H.; Tang, Y.; Yuan, Y.; Liu, Y.; Oil and gas survey, China Geological Survey, Ministry of Natural Resources; et al. Geological Characteristics and Co-Exploration and Co-Production Methods of Upper Permian Longtan Coal Measure Gas in Yangmeishu Syncline, Western Guizhou Province, China. *China Geol.* **2020**, *3*, 38–51. [CrossRef]
8. Li, Z.; Ripepi, N.; Chen, C. Using Pressure Pulse Decay Experiments and a Novel Multi-Physics Shale Transport Model to Study the Role of Klinkenberg Effect and Effective Stress on the Apparent Permeability of Shales. *J. Pet. Sci. Eng.* **2020**, *189*, 107010. [CrossRef]
9. Fu, H.; Tang, D.; Xu, H.; Xu, T.; Chen, B.; Hu, P.; Yin, Z.; Wu, P.; He, G. Geological Characteristics and CBM Exploration Potential Evaluation: A Case Study in the Middle of the Southern Junggar Basin, NW China. *J. Nat. Gas Sci. Eng.* **2016**, *30*, 557–570. [CrossRef]
10. Zhang, S.; Tang, S.; Zhang, J.; Pan, Z. Pore Structure Characteristics of China Sapropelic Coal and Their Development Influence Factors. *J. Nat. Gas Sci. Eng.* **2018**, *53*, 370–384. [CrossRef]
11. Fu, H.; Tang, D.; Xu, T.; Xu, H.; Tao, S.; Li, S.; Yin, Z.; Chen, B.; Zhang, C.; Wang, L. Characteristics of Pore Structure and Fractal Dimension of Low-Rank Coal: A Case Study of Lower Jurassic Xishanyao Coal in the Southern Junggar Basin, NW China. *Fuel* **2017**, *193*, 254–264. [CrossRef]
12. Liu, Z.; Yang, H.; Wang, W.; Cheng, W.; Xin, L. Experimental Study on the Pore Structure Fractals and Seepage Characteristics of a Coal Sample around a Borehole in Coal Seam Water Infusion. *Transp. Porous Med.* **2018**, *125*, 289–309. [CrossRef]
13. Li, Z.; Zhao, Q.; Teng, Y.; Fan, M.; Ripepi, N.; Yin, X.; Chen, C. Experimental Investigation of Non-Monotonic Fracture Conductivity Evolution in Energy Georeservoirs. *J. Pet. Sci. Eng.* **2022**, *211*, 110103. [CrossRef]
14. Zhang, L.; Kou, Z.; Wang, H.; Zhao, Y.; Dejam, M.; Guo, J.; Du, J. Performance Analysis for a Model of a Multi-Wing Hydraulically Fractured Vertical Well in a Coalbed Methane Gas Reservoir. *J. Pet. Sci. Eng.* **2018**, *166*, 104–120. [CrossRef]
15. Luo, Q.; Xiao, Z.; Dong, C.; Ye, X.; Li, H.; Zhang, Y.; Ma, Y.; Ma, L.; Xu, Y. The Geochemical Characteristics and Gas Potential of the Longtan Formation in the Eastern Sichuan Basin, China. *J. Pet. Sci. Eng.* **2019**, *179*, 1102–1113. [CrossRef]
16. Wu, Z.; He, S.; Han, Y.; Zhai, G.; He, X.; Zhou, Z. Effect of Organic Matter Type and Maturity on Organic Matter Pore Formation of Transitional Facies Shales: A Case Study on Upper Permian Longtan and Dalong Shales in Middle Yangtze Region, China. *J. Earth Sci.* **2020**, *31*, 368–384. [CrossRef]
17. He, Q.; Dong, T.; He, S.; Zhai, G. Methane Adsorption Capacity of Marine-Continental Transitional Facies Shales: The Case Study of the Upper Permian Longtan Formation, Northern Guizhou Province, Southwest China. *J. Pet. Sci. Eng.* **2019**, *183*, 106406. [CrossRef]
18. Zhao, L.; Guanhua, N.; Lulu, S.; Qian, S.; Shang, L.; Kai, D.; Jingna, X.; Gang, W. Effect of Ionic Liquid Treatment on Pore Structure and Fractal Characteristics of Low Rank Coal. *Fuel* **2020**, *262*, 116513. [CrossRef]
19. Tsakiroglou, C.D.; Payatakes, A.C. Characterization of the Pore Structure of Reservoir Rocks with the Aid of Serial Sectioning Analysis, Mercury Porosimetry and Network Simulation. *Adv. Water Resour.* **2000**, *23*, 773–789. [CrossRef]
20. Zhang, J.; Li, X.; Wei, Q.; Sun, K.; Zhang, G.; Wang, F. Characterization of Full-Sized Pore Structure and Fractal Characteristics of Marine–Continental Transitional Longtan Formation Shale of Sichuan Basin, South China. *Energy Fuels* **2017**, *31*, 10490–10504. [CrossRef]
21. Wang, H.; Kou, Z.; Guo, J.; Chen, Z. A Semi-Analytical Model for the Transient Pressure Behaviors of a Multiple Fractured Well in a Coal Seam Gas Reservoir. *J. Pet. Sci. Eng.* **2021**, *198*, 108159. [CrossRef]

22. Wood, D.A. Deriving Coal Fractal Dimensions from Low-Pressure Nitrogen Adsorption Isotherms Applying an Integrated Method. *Appl. Geochem.* **2021**, *131*, 105042. [CrossRef]
23. Liu, S.; Tang, S.; Yin, S. Coalbed Methane Recovery from Multilateral Horizontal Wells in Southern Qinshui Basin. *Adv. Geo-Energy Res.* **2018**, *2*, 34–42. [CrossRef]
24. Mahamud, M.M.; Novo, M.F. The Use of Fractal Analysis in the Textural Characterization of Coals. *Fuel* **2008**, *87*, 222–231. [CrossRef]
25. Cai, Y.; Liu, D.; Yao, Y.; Li, J.; Liu, J. Fractal Characteristics of Coal Pores Based on Classic Geometry and Thermodynamics Models. *Acta Geol. Sin.-Engl. Ed.* **2011**, *85*, 1150–1162. [CrossRef]
26. Andhumoudine, A.B.; Nie, X.; Zhou, Q.; Yu, J.; Kane, O.I.; Jin, L.; Djaroun, R.R. Investigation of Coal Elastic Properties Based on Digital Core Technology and Finite Element Method. *Adv. Geo-Energy Res.* **2021**, *5*, 53–63. [CrossRef]
27. Zhang, Q.; Grohmann, S.; Xu, X.; Littke, R. Depositional Environment and Thermal Maturity of the Coal-Bearing Longtan Shale in Southwest Guizhou, China: Implications for Shale Gas Resource Potential. *Int. J. Coal Geol.* **2020**, *231*, 103607. [CrossRef]
28. Kou, Z.; Wang, T.; Chen, Z.; Jiang, J. A Fast and Reliable Methodology to Evaluate Maximum CO_2 Storage Capacity of Depleted Coal Seams: A Case Study. *Energy* **2021**, *231*, 120992. [CrossRef]
29. Pan, J.; Zhang, Z.; Li, M.; Wu, Y.; Wang, K. Characteristics of Multi-Scale Pore Structure of Coal and Its Influence on Permeability. *Nat. Gas Ind. B* **2019**, *6*, 357–365. [CrossRef]
30. Yang, C.; Xiong, Y.; Zhang, J.; Liu, Y.; Chen, C. Comprehensive Understanding of OM-Hosted Pores in Transitional Shale: A Case Study of Permian Longtan Shale in South China Based on Organic Petrographic Analysis, Gas Adsorption, and X-Ray Diffraction Measurements. *Energy Fuels* **2019**, *33*, 8055–8064. [CrossRef]
31. Yang, X.; Ren, T.; He, X. Experimental Study of Coal Burst Risk Prediction Using Fractal Dimension Analysis of AE Spatial Distribution. *J. Appl. Geophys.* **2020**, *177*, 104025. [CrossRef]
32. Cheng, J.; Zhou, J.; Li, Y.; Liu, J.; Cen, K. Effects of Pore Fractal Structures of Ultrafine Coal Water Slurries on Rheological Behaviors and Combustion Dynamics. *Fuel* **2008**, *87*, 2620–2627. [CrossRef]
33. Zhou, Q.; Qin, B.; Wang, J.; Wang, H.; Wang, F. Experimental Investigation on the Changes of the Wettability and Surface Characteristics of Coal Dust with Different Fractal Dimensions. *Colloids Surf. A Physicochem. Eng. Asp.* **2018**, *551*, 148–157. [CrossRef]
34. Wang, Z.; Cheng, Y.; Qi, Y.; Wang, R.; Wang, L.; Jiang, J. Experimental Study of Pore Structure and Fractal Characteristics of Pulverized Intact Coal and Tectonic Coal by Low Temperature Nitrogen Adsorption. *Powder Technol.* **2019**, *350*, 15–25. [CrossRef]
35. Faulon, J.-L.; Mathews, J.P.; Carlson, G.A.; Hatcher, P.G. Correlation between Microporosity and Fractal Dimension of Bituminous Coal Based on Computer-Generated Models. *Energy Fuels* **1994**, *8*, 408–414. [CrossRef]
36. Mondal, D.; Roy, P.N.S.; Behera, P.K. Use of Correlation Fractal Dimension Signatures for Understanding the Overlying Strata Dynamics in Longwall Coal Mines. *Int. J. Rock Mech. Min. Sci.* **2017**, *91*, 210–221. [CrossRef]
37. Reich, M.H.; Snook, I.K.; Wagenfeld, H.K. A Fractal Interpretation of the Effect of Drying on the Pore Structure of Victorian Brown Coal. *Fuel* **1992**, *71*, 669–672. [CrossRef]
38. Mendhe, V.A.; Bannerjee, M.; Varma, A.K.; Kamble, A.D.; Mishra, S.; Singh, B.D. Fractal and Pore Dispositions of Coal Seams with Significance to Coalbed Methane Plays of East Bokaro, Jharkhand, India. *J. Nat. Gas Sci. Eng.* **2017**, *38*, 412–433. [CrossRef]
39. Cai, Y.; Liu, D.; Pan, Z.; Che, Y.; Liu, Z. Investigating the Effects of Seepage-Pores and Fractures on Coal Permeability by Fractal Analysis. *Transp. Porous Med.* **2016**, *111*, 479–497. [CrossRef]
40. Yin, T.; Liu, D.; Cai, Y.; Zhou, Y.; Yao, Y. Size Distribution and Fractal Characteristics of Coal Pores through Nuclear Magnetic Resonance Cryoporometry. *Energy Fuels* **2017**, *31*, 7746–7757. [CrossRef]
41. Huang, F.; Cao, Z.; Guo, J.; Jiang, S.-H.; Li, S.; Guo, Z. Comparisons of Heuristic, General Statistical and Machine Learning Models for Landslide Susceptibility Prediction and Mapping. *CATENA* **2020**, *191*, 104580. [CrossRef]
42. Huang, F.; Chen, J.; Liu, W.; Huang, J.; Hong, H.; Chen, W. Regional Rainfall-Induced Landslide Hazard Warning Based on Landslide Susceptibility Mapping and a Critical Rainfall Threshold. *Geomorphology* **2022**, *408*, 108236. [CrossRef]
43. Li, H.; Shi, S.; Lu, J.; Ye, Q.; Lu, Y.; Zhu, X. Pore Structure and Multifractal Analysis of Coal Subjected to Microwave Heating. *Powder Technol.* **2019**, *346*, 97–108. [CrossRef]
44. Chang, Z.; Du, Z.; Zhang, F.; Huang, F.; Chen, J.; Li, W.; Guo, Z. Landslide Susceptibility Prediction Based on Remote Sensing Images and GIS: Comparisons of Supervised and Unsupervised Machine Learning Models. *Remote Sens.* **2020**, *12*, 502. [CrossRef]
45. Li, Z.; Teng, Y.; Fan, M.; Ripepi, N.; Chen, C. A Novel Multiphysics Multiscale Multiporosity Shale Gas Transport Model for Geomechanics/Flow Coupling in Steady and Transient States. *SPE J.* **2022**, *27*, 452–464. [CrossRef]
46. Deng, E.; Zhang, Q.; Jin, Z.; Zhu, R.; Yan, Z.; Jiang, B.; Littke, R. Non-Overmature Equivalents Confirmed a High Initial Hydrocarbon Generation Potential of the Permian Longtan Shale in Southern China. *Int. J. Coal Geol.* **2022**, *259*, 104043. [CrossRef]
47. Liu, X.; Nie, B. Fractal Characteristics of Coal Samples Utilizing Image Analysis and Gas Adsorption. *Fuel* **2016**, *182*, 314–322. [CrossRef]
48. Fu, X.; Qin, Y.; Zhang, W.; Wei, C.; Zhou, R. Fractal Classification and Natural Classification of Coal Pore Structure Based on Migration of Coal Bed Methane. *Chin. Sci. Bull.* **2005**, *50*, 66–71. [CrossRef]
49. Huang, F.; Cao, Z.; Jiang, S.-H.; Zhou, C.; Huang, J.; Guo, Z. Landslide Susceptibility Prediction Based on a Semi-Supervised Multiple-Layer Perceptron Model. *Landslides* **2020**, *17*, 2919–2930. [CrossRef]

50. Jiang, S.-H.; Huang, J.; Huang, F.; Yang, J.; Yao, C.; Zhou, C.-B. Modelling of Spatial Variability of Soil Undrained Shear Strength by Conditional Random Fields for Slope Reliability Analysis. *Appl. Math. Model.* **2018**, *63*, 374–389. [CrossRef]
51. Huang, F.; Zhang, J.; Zhou, C.; Wang, Y.; Huang, J.; Zhu, L. A Deep Learning Algorithm Using a Fully Connected Sparse Autoencoder Neural Network for Landslide Susceptibility Prediction. *Landslides* **2020**, *17*, 217–229. [CrossRef]
52. Chang, Z.; Catani, F.; Huang, F.; Liu, G.; Meena, S.R.; Huang, J.; Zhou, C. Landslide Susceptibility Prediction Using Slope Unit-Based Machine Learning Models Considering the Heterogeneity of Conditioning Factors. *J. Rock Mech. Geotech. Eng.* **2022**, S1674775522001615. [CrossRef]
53. Ju, Y.; Luxbacher, K.; Li, X.; Wang, G.; Yan, Z.; Wei, M.; Yu, L. Micro-Structural Evolution and Their Effects on Physical Properties in Different Types of Tectonically Deformed Coals. *Int. J. Coal Sci. Technol.* **2014**, *1*, 364–375. [CrossRef]
54. Cai, Y.; Li, Q.; Liu, D.; Zhou, Y.; Lv, D. Insights into Matrix Compressibility of Coals by Mercury Intrusion Porosimetry and N2 Adsorption. *Int. J. Coal Geol.* **2018**, *200*, 199–212. [CrossRef]
55. Yang, Q.; Xue, J.; Li, W.; Du, X.; Ma, Q.; Zhan, K.; Chen, Z. Comprehensive Evaluation and Interpretation of Mercury Intrusion Porosimetry Data of Coals Based on Fractal Theory, Tait Equation and Matrix Compressibility. *Fuel* **2021**, *298*, 120823. [CrossRef]
56. Yao, Y.; Liu, D.; Tang, D.; Tang, S.; Huang, W.; Liu, Z.; Che, Y. Fractal Characterization of Seepage-Pores of Coals from China: An Investigation on Permeability of Coals. *Comput. Geosci.* **2009**, *35*, 1159–1166. [CrossRef]
57. Qin, L.; Zhai, C.; Liu, S.; Xu, J.; Wu, S.; Dong, R. Fractal Dimensions of Low Rank Coal Subjected to Liquid Nitrogen Freeze-Thaw Based on Nuclear Magnetic Resonance Applied for Coalbed Methane Recovery. *Powder Technol.* **2018**, *325*, 11–20. [CrossRef]
58. Liu, L.; Cui, Z.; Wang, J.; Xia, Z.; Duan, L.; Yang, Y.; Li, M.; Li, T. Pore Size Distribution Characteristics of High Rank Coal with Various Grain Sizes. *ACS Omega* **2020**, *5*, 19785–19795. [CrossRef]